Binding of Six Nucleotide Cofactors to the Hexameric Helicase RepA Protein of Plasmid RSF1010. 2. Base Specificity, Nucleotide Structure, Magnesium, and Salt Effect on the Cooperative Binding of the Cofactors†

Maria J. Jezewska, Aaron L. Lucius, and Wlodzimierz Bujalowski*

Department of Human Biological Chemistry and Genetics, Department of Obstetrics and Gynecology, the Sealy Center for Structural Biology, Sealy Center for Cancer Cell Biology, The University of Texas Medical Branch at Galveston, 301 University Boulevard, Galveston, Texas 77555-1053

Received September 10, 2004; Revised Manuscript Received December 15, 2004

ABSTRACT: Interactions of the RepA hexameric helicase with nucleotide cofactors have been examined using nucleotide analogues, TNP-ADP and TNP-ATP, and unmodified nucleotides. Thermodynamic parameters for the interactions of modified and unmodified nucleotides have been obtained using quantitative fluorescence titration and competition titration methods. The intrinsic binding constant of ATP is by a factor of ∼10 and ∼1000 higher than the value observed for ADP and PO_4^-. The data suggest that helicase acquires free-energy transducing capabilities when associated with the ssDNA, thus, forming a "holoenzyme". ATP binding is characterized by significantly stronger negative cooperativity than ADP. The cooperative interactions are predominantly induced through the specific interactions of the γ phosphate and the ribose with the protein. The salt effect on cofactor binding indicates a very different nature of the intrinsic and cooperative interactions. Surprisingly, binding of Mg^{2+}, to both the cofactor and helicase, predominantly controls the ADP−RepA interactions. Mg^{2+} cations seem to play a role in affecting the distribution of high and low ssDNA-affinity states, through the strong effect on the diphosphate versus triphosphate binding. The data indicate that Mg^{2+} has a dual function in nucleotide−helicase interactions. At low [Mg^{2+}], NTP binds stronger than NDP and the enzyme is predominantly in the high ssDNA-affinity state. At higher [Mg^{2+}], NTP binds weaker than NDP and the helicase subunits can exist in alternating low- and high-affinity states that facilitate the efficient dsDNA unwinding. The RepA helicase shows a preference toward purine nucleotides. The cooperative interactions are independent of the type of the base.

The RepA protein is a hexameric DNA replicative helicase that is essential for replication of the RFS1010 plasmid, a broad host nonconjugative plasmid that can replicate in most Gram-negative bacteria and confers bacterial resistance to sulfonamides and streptomycin (accompanying paper 1, *1*−*8*). The protein forms a very stable, ring-like hexameric structure in the absence of any cofactors or salt in solution (*3*, *5*, *6*). This property differs the RepA helicase from other well-known hexameric enzymes such as bacteriophage T7 and T4 helicase but resembles the stable hexamer of the *Escherichia coli* DnaB replicative hexameric helicase, which requires only magnesium cations to maintain its structure (*10*−*14*). The RepA hexamer has a diameter of ∼140 Å, while the diameter of the central cross channel of the ring-like structure of the enzyme is only ∼17 Å (*4*−*5*).

In the reaction of the dsDNA unwinding catalyzed by helicases, the enzymes perform a complex free-energy transduction process (*15*−*17*). However, the mechanism of the binding and/or hydrolysis of NTPs, as well as the regulation of the enzyme activity and affinity toward the nucleic acid are not yet completely understood for any helicase. In the accompanying paper 1, we have quantitatively examined the binding of the analogues of nucleotide cofactor, 2′(3′)-*O*-(2,4,6-trinitrophenyl)adenosine-5′-diphosphate (TNP-ADP),[1] 2′(3′)-*O*-(2,4,6-trinitrophenyl)adenosine-5′-triphosphate (TNP-ATP), and MANT-ADP to the RepA hexamer. The analysis has been facilitated by the fact that binding of the analogues is accompanied by a large quenching of the protein fluorescence, predominantly because of the fluorescence energy transfer from protein tryptophans to the TNP or MANT moiety, indicating that the tryptophans are in close proximity to the nucleotide-binding sites. The RepA hexamer binds six molecules of TNP-ADP or TNP-ATP; thus, all presumed nucleotide-binding sites of the RepA helicase can actively engage in binding of nucleotide cofactors. However, the macroscopic affinity of the binding

† This work was supported by NIH Grant R01 GM-46679 (to W.B.).

* To whom correspondence should be addressed: Department of Human Biological Chemistry and Genetics, The University of Texas Medical Branch at Galveston, 301 University Boulevard, Galveston, TX 77555-1053. Telephone: (409) 772-5634. Fax: (409) 772-1790. E-mail: wbujalow@utmb.edu.

[1] Abbreviations: ATPγS, adenosine-5′-*O*-(3-thiotriphosphate); AMP-PNP, β,γ-imodoadenosine-5′-triphosphate; AMP-PCP, β,γ-methylenadenosine-5′-triphosphate; TNP-ATP, 2′(3′)-*O*-(2,4,6-trinitrophenyl)adenosine-5′-triphosphate; TNP-ADP, 2′(3′)-*O*-(2,4,6-trinitrophenyl)adenosine-5′-diphosphate; ADP, adenosine-5′-diphosphate; GDP, guanosine-5′-diphosphate; CDP, cytosine-5′-diphosphate; TDP, thymidine-5′-diphosphate; Tris, tris(hydroxymethyl)aminomethane.

10.1021/bi048036h CCC: $30.25
Published on Web 02/15/2005

process decreases with the increase of the average degree of binding of the cofactors. Such behavior indicates, independently of any binding model, the existence of significant heterogeneity in the affinity among the nucleotide-binding sites of the RepA hexamer. The observed heterogeneity in affinity reflects the negative cooperative interactions between the binding sites. A statistical thermodynamic model, the hexagon model, provides an excellent description of the binding isotherms and the dependence of the observed fluorescence quenching as a function of the average degree of binding, using only two interaction parameters, the intrinsic binding constant, K, and the cooperativity parameter, σ.

The obtained data and analyses of the nucleotide binding to the RepA hexamer exclude the alternative model of two independent classes of independent binding sites, often invoked in interpretation of the nucleotide binding to the hexameric helicases (*8*, *18*). The model of two independent classes of independent binding sites cannot account for both, the binding isotherm and the dependence of the fluorescence quenching upon the average degree of binding. This inability results from the fact that the model imposes a strict requirement of additivity of the partial spectroscopic parameters (fluorescence quenching), characterizing the nucleotide binding to the sites in each class of binding sites, in all possible complexes of a cofactor with the hexamer. On the other hand, the hexagon model is not limited by any strict requirement for the additivity of the partial spectroscopic parameters.

In this paper, which is a logical continuation of the first paper in this series, we describe extensive analyses of the RepA hexamer interactions with several modified and unmodified nucleotide cofactors, inorganic phosphate, and the role of salt and magnesium in these interactions, using the quantitative fluorescence titration technique (accompanying paper 1) and the competition titration methods (*19*−*23*).

MATERIALS AND METHODS

Reagents and Buffers. All chemicals were reagent-grade. All solutions were made with distilled and deionized >18 MΩ (Milli-Q Plus) water as described in accompanying paper 1. The temperature and concentrations of NaCl and $MgCl_2$ in the buffer are indicated in the text.

RepA Helicase of Plasmid RSF1010. Isolation and purification of the RepA protein was performed, as described in accompanying paper 1 (*3*). The concentration of the protein was spectrophotometrically determined using the extinction coefficient $\epsilon_{280} = 1.66 \times 10^5$ cm^{-1} M^{-1}, obtained with the approach based on Edelhoch's method (*24*, *25*).

Nucleotides. TNP-ATP and TNP-ADP were from Molecular Probes (Eugene, OR). ATP was from CalBiochem. Adenosine-5′-diphosphate (ADP), dATP, dADP, guanosine-5′-diphosphate (GDP), thymidine-5′-diphosphate (TDP), cytosine-5′-diphosphate (CDP), and UDP were from Sigma.

Fluorescence Measurements. All steady-state fluorescence titrations were performed using the SLM-AMINCO 8100C as described in accompanying paper 1 (*20*−*29*).

Quantitative Determination of Binding Isotherms and Stoichiometries of the RepA Hexamer−*Nucleotide Cofactor Complexes*. Quantitative estimates of the average degree of binding, $\sum\Theta_i$ (number of nucleotide molecules bound per RepA hexamer), and the free nucleotide concentration, P_F, were obtained as described in accompanying paper 1 (*19*−*23*). The analysis of a single binding isotherm, without the necessity of determining all fluorescence parameters for different complexes, has been performed using the empirical function method (accompanying paper 1) (*23*, *30*). For the empirical function that relates the experimentally determined dependence of the RepA protein fluorescence quenching, ΔF_{obs}, to the average degree of binding, $\sum\Theta_i$, a polynomial function has been selected as

$$\Delta F_{obs} = \sum_{j=0}^{n} a_j \left(\sum \Theta_i\right)^j \quad (1)$$

where a_j values are fitting constants (*23*, *30*).

RESULTS

Binding of Unmodified ATP, ADP, and Inorganic Phosphate to the RepA Hexamer. As pointed out in accompanying paper 1, the binding of ATP and ADP to the RepA protein is not accompanied by a protein fluorescence change adequate to quantitatively determine the energetics of the interactions. On the other hand, interactions of the unmodified ATP and ADP with the RepA hexamer can be quantitatively determined using a competition titration method, described before by us (*20*, *21*). In this approach, the protein is titrated with the reference nucleotide analogue, e.g., TNP-ADP, in the absence and presence of the unmodified nucleotide. The observed signal originates only from the binding of the "reference" cofactor; however, the titration curve, in the presence of unmodified nucleotide, is shifted to higher reference nucleotide concentrations, because of the competition with the unmodified cofactor (*20*, *21*, *23*).

Fluorescence titrations of RepA helicase with the TNP-ADP in the absence and presence of 3 mM ADP in buffer T5 (at pH 7.6 and 10 °C), containing 10 mM NaCl and 5 mM $MgCl_2$, are shown in Figure 1a. The concentration of the RepA protein is 1×10^{-6} M (hexamer). The presence of ADP shifts the titration curves toward a higher TNP-ADP concentration range, clearly indicating that both nucleotides compete for the same binding sites on the RepA hexamer. There are two important qualitative aspects of these data. First, despite the large concentration of ADP (3 mM), the shift of the isotherm to the higher TNP-ADP concentration range is only moderate, as compared to the isotherm recorded in the absence of ADP, indicating that ADP has a much lower affinity than TNP-ADP for the nucleotide-binding sites of the RepA hexamer. Second, inspection of the plot shows that the shift of the isotherm is not symmetric; i.e., it is larger at higher [TNP-ADP]. Such an asymmetric shift of the isotherm in the presence of the competing ligand indicates that cooperative interactions between TNP-ADP and ADP and/or between ADP molecules bound to the RepA hexamer are different from cooperative interactions between the reference TNP-ADP molecules (*20*, *21*, *23*) (see below).

The RepA helicase alone does not hydrolyze ATP on the time scale of the binding experiment, to any significant extent, in the applied solution conditions (buffer T5 at pH 7.6 and 10 °C). Such behavior allowed us to perform the same competition binding analysis using unmodified ATP. Fluorescence titration of RepA helicase with the TNP-ADP

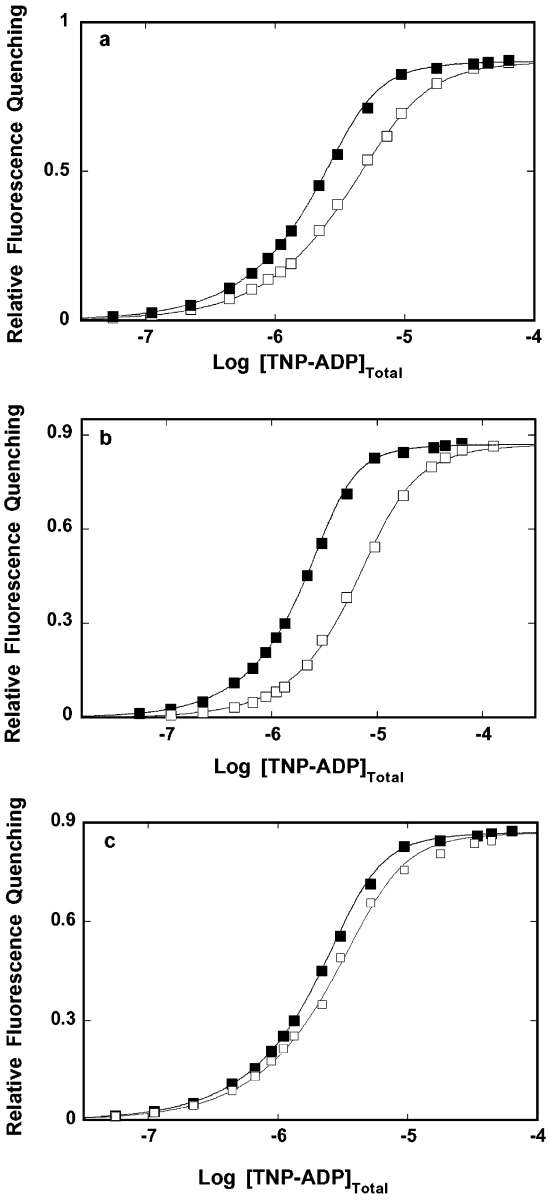

FIGURE 1: (a) Fluorescence titration of the RepA helicase with TNP-ADP in buffer T5 (at pH 7.6 and 10 °C), containing 10 mM NaCl and 5 mM $MgCl_2$, in the absence (■) and the presence (□) of 3 mM ADP. The solid lines are nonlinear least-square fits of the titration curves, according to the hexagon model for two competing ligands (eqs 2−4) and the empirical function defined by eq 5, using binding parameters for ADP included in Table 1. The intrinsic binding constant of the reference nucleotide, TNP-ADP, is $K = 1 \times 10^7$ M^{-1} and cooperativity parameter $\sigma = 0.3$. (b) Fluorescence titration of the RepA helicase with TNP-ADP in buffer T5 (at pH 7.6 and 10 °C), containing 10 mM NaCl and 5 mM $MgCl_2$, in the absence (■) and presence (□) of 3 mM ATP. The solid lines are nonlinear least-square fits of the titration curves, according to the hexagon model for two competing ligands (eqs 2−4) and the empirical function defined by eq 5, using binding parameters for ATP included in Table 1. (c) Fluorescence titration of the RepA helicase with TNP-ADP in the same solution condition as the titration performed in the presence of ADP and ATP in a and b, in the absence (■) and presence (□) of 50 mM K_2HPO_4. The solid lines are nonlinear least-square fits of the titration curves, according to the hexagon model for two competing ligands (eqs 2−4) and the empirical function defined by eq 5, using binding parameters for the inorganic phosphate included in Table 1. In a−c, the concentration of the RepA helicase is 1×10^{-6} M (hexamer).

in the presence of 3 mM ATP in buffer T5 (at pH 7.6 and 10 °C), containing 10 mM NaCl and 5 mM $MgCl_2$, together with the titration of the RepA protein with TNP-ADP in the absence of ATP, are shown in Figure 1b. The concentration of the RepA protein is the same as applied in ADP binding experiments (Figure 1a). In the presence of ATP, the titration curve is shifted to a higher concentration range of TNP-ADP than that observed in the presence of ADP, indicating that ATP has a higher macroscopic affinity for the nucleotide-binding site of the helicase than adenosine diphosphate. Analogous fluorescence titration of the RepA helicase with TNP-ADP in the presence of 50 mM K_2PO_4 is shown in Figure 1c. The concentration of K_2PO_4 has been selected on the basis of the fact that the increase of the salt concentration up to ~100 mM NaCl does not significantly affect the TNP-ADP affinity of the RepA helicase (see below). It is evident that the presence of 50 mM K_2PO_4 induces only a modest shift of the titration curve toward higher [TNP-ADP], indicating a substantially lower macroscopic affinity of the phosphate group for the nucleotide-binding site than observed for ADP and ATP (see the Discussion).

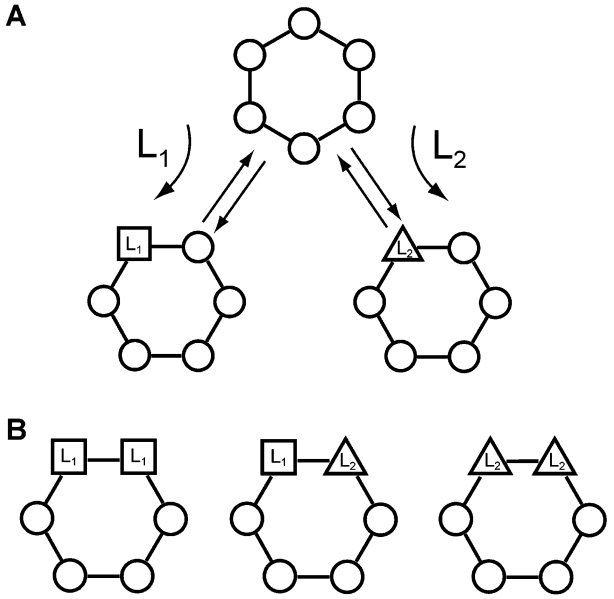

FIGURE 2: Schematic model of the hexagon lattice of the RepA hexamer (A) with the three, possible different states of each lattice site: free (○), bound with a reference ligand, L_R (□), and bound with the competing ligand, L_C (△). Three different types of possible cooperative interactions (B) between the ligand molecules, bound to neighboring sites of the hexamer and characterized by corresponding cooperativity parameters; reference ligand molecules, L1, characterized by cooperativity parameter, σ; competing ligand molecules (L2) characterized by cooperativity parameter, σ_C reference and competing ligand molecules (L1 and L2) characterized by cooperativity parameter, σ_{RC}.

Statistical Thermodynamic Analysis of the Competitive Cooperative Ligand Binding to a Circular Lattice. In general, in the presence of the reference ligand, TNP-ADP, and competing unmodified ligand, e.g., ADP, each nucleotide-binding site of the RepA hexamer can exist in three different states, free, bound with TNP-ADP, or bound with the unmodified nucleotide. The schematic representation of the different types of states and interactions in the competitive binding of two ligands to a circular lattice with six binding sites, according to the hexagon model for both ligands, is shown in Figure 2.

Analytical extension of the hexagon model to such a complex system (accompanying paper 1) can be most

Table 1: Maximum Number of Binding Sites, n, Intrinsic Binding Constant, K_{in}, Cooperativity Parameter, σ, for the Binding of the Ribose and Deoxyribose Nucleoside Tri- and Diphosphates and Inorganic Phosphate to the RSF1010 RepA Hexameric Helicase in Buffer T2 (at pH 7.6 and 10 °C) Containing 10 mM NaCl and 5 mM $MgCl_2$

parameter	ATP	dATP	ADP	dADP	PO_4^-
n	6	6	6	6	6
K_C (M^{-1})	$(1.9 \pm 0.5) \times 10^5$	$(9.8 \pm 1.5) \times 10^4$	$(1.43 \pm 0.8) \times 10^4$	$(3.7 \pm 1) \times 10^4$	$(2.5 \pm 0.5) \times 10^2$
σ_C	0.003 ± 0.0005	0.085 ± 0.021	0.17 ± 0.03	0.12 ± 0.04	0.15 ± 0.09
σ_{RC}	0.11 ± 0.02	0.16 ± 0.02	0.25 ± 0.05	0.23 ± 0.05	0.25 ± 0.04

efficiently handled by the matrix method to obtain the expressions for the partition function, Z_H, and the average degree of binding, $\sum\Theta_i$, of the reference nucleotide, in terms of its intrinsic binding parameters and the intrinsic binding parameters of the unmodified competing nucleotide (*21*, *31*). The transfer matrix M, that correlates the statistical weights of different states of the nucleotide−hexamer complex, is a three-state matrix, defined as (*21*)

$$\mathrm{M}=\begin{pmatrix} 1 & KL_R & K_CL_C \\ 1 & \sigma KL_R & \sigma_{RC}K_CL_C \\ 1 & \sigma_{RC}KL_R & \sigma_C K_C L_C \end{pmatrix} \quad (2)$$

where K is the intrinsic binding constant of the reference modified nucleotide (TNP-ADP), L_R is the free concentration of the reference nucleotide, σ is the parameter characterizing cooperative interactions between bound reference nucleotide molecules, K_C is the intrinsic binding constant of the unmodified competing nucleotide, L_C is the free concentration of the unmodified competing nucleotide, σ_C is the parameter characterizing cooperative interactions between unmodified competing nucleotide molecules, and σ_{RC} is the parameter characterizing cooperative interactions between the reference and the unmodified competing nucleotide, respectively. The partition function of the entire binding system is then

$$Z_H = (1\ 0\ 0)\ \mathrm{M}^6\begin{pmatrix}1\\0\\0\end{pmatrix} + (0\ 1\ 0)\ \mathrm{M}^6\begin{pmatrix}0\\1\\0\end{pmatrix} + (0\ 0\ 1)\ \mathrm{M}^6\begin{pmatrix}0\\0\\1\end{pmatrix} \quad (3)$$

The average degree of binding of the reference nucleotide (TNP-ADP), $\sum\Theta_i$, is defined by the standard thermodynamic relationship, ∂ Ln Z_H/ ∂ Ln L_R, which provides (*21*)

$$\sum\Theta_i = \frac{\left[(1\ 0\ 0)\dfrac{\partial\,\mathrm{M}^6}{\partial \ln \mathrm{L_R}}\begin{pmatrix}1\\0\\0\end{pmatrix} + (0\ 1\ 0)\left[\dfrac{\partial\,\mathrm{M}^6}{\partial \ln \mathrm{L_R}}\right]\begin{pmatrix}0\\1\\0\end{pmatrix} + (0\ 0\ 1)\left[\dfrac{\partial\,\mathrm{M}^6}{\partial \ln \mathrm{L_R}}\right]\begin{pmatrix}0\\0\\1\end{pmatrix}\right]}{Z_h} \quad (4)$$

Notice, there are five parameters in eqs 1−4, K, σ, K_C, σ_C, and σ_{RC}. However, K and σ are independently determined from fluorescence titration of the RepA hexamer with TNP-ADP in the absence of the competing unmodified nucleotide (accompanying paper 1). Therefore, there are only three parameters, K_C, σ_C, and σ_{RC}, which can be determined by nonlinear least-squares fitting of the experimental titration curves.

The solid lines in parts a−c of Figure 1 are nonlinear least-square fits of the spectroscopic binding curves using eqs 1−4 and the empirical function (eq 1) that describes the experimentally obtained dependence of ΔF_{obs} as a function of $\sum\Theta_i$ (accompanying paper 1). In the applied solution conditions, this function is defined as

$$\Delta F_{obs} = 2.6054 \times 10^1\left(\sum\Theta_i\right) - 1.9224 \times 10^2\left(\sum\Theta_i\right)^2 \quad (5)$$

The intrinsic binding constant, K, and the cooperativity parameter, σ, for the TNP-ADP binding to the RepA helicase, in the same solution conditions, are 1×10^7 M^{-1} and 0.3, respectively (see below). The binding parameters for ADP, ATP, and inorganic phosphate are included in Table 1.

The obtained data show that ATP has an intrinsic affinity of approximately an order of magnitude higher than ADP. However, binding of ATP to the RepA hexamer is characterized by the cooperativity parameter $\sigma = 0.003 \pm 0.0005$ as compared to $\sigma = 0.17 \pm 0.03$ for ADP, i.e., a factor of ~57 lower, indicating that the adenosine triphosphate binds with much higher negative cooperativity than ADP. The intrinsic affinity of inorganic phosphate is characterized by $K = (2.5 \pm 0.5) \times 10^2$ M^{-1}, approximately 3 and 2 orders of magnitude lower than the intrinsic binding constant obtained for ATP and ADP, respectively (Table 1). On the other hand, the cooperativity parameter for the inorganic phosphate binding, $\sigma = 0.15 \pm 0.05$, is very similar to the value of the same parameter obtained for ADP (see the Discussion).

Base Specificity of the Nucleotide-Binding Site of the RepA Helicase. Ligand competition studies can provide direct quantitative estimates of the base specificity of the nucleotide-binding site of the RepA helicase (*20*, *21*, *32*). Fluorescence titrations of the RepA protein with TNP-ADP in the presence of 3 mM GTP or 3 mM TDP, in buffer T5 (at pH 7.6 and 10 °C), containing 10 mM NaCl and 5 mM $MgCl_2$, are shown in Figure 3. For comparison, the titration of the RepA protein with TNP-ADP, in the absence of competing cofactors, is also included. The titration curve is shifted to higher concentrations of TNP-ADP in the presence of GDP than TDP, indicating that, independently of any binding model, GDP competes more efficiently with TNP-ADP for the nucleotide-binding sites of the RepA hexamer than TDP. The solid lines in Figure 3 are nonlinear least-squares fits of the experimental titration curves according to the hexagon model of two competing, cooperatively binding ligands, using eqs 1−4 and the empirical function defined by eq 5. Analogous titrations and analyses have been performed for a series of nucleotide cofactors, and the corresponding binding parameters for all examined nucleotides are included in Table 2. The affinity of UDP is too low to reliably estimate its cooperativity parameter. Nevertheless, the obtained data clearly indicate that the nucleotide-binding site of the RepA helicase has a preference for the purine nucleotides, with the affinities of the ADP and GDP

Table 2: Maximum Number of Binding Sites, n, Intrinsic Binding Constant, K_{in}, Cooperativity Parameter, σ, for the Binding of the Nucleoside Tri- and Diphosphates to the RSF1010 RepA Hexameric Helicase in Buffer T2 (at pH 7.6 and 10 °C) Containing 10 mM NaCl and 5 mM $MgCl_2$

parameter	ATPγS	AMP-PNP	AMP-PCP	GDP	TDP	CDP	UDP
n	6	6	6	6	6	6	6
K_C (M^{-1})	$(8.8 \pm 2.1) \times 10^4$	$(2.2 \pm 0.7) \times 10^4$	$(1 \pm 0.3) \times 10^3$	$(3.0 \pm 1) \times 10^4$	$(5 \pm 1.3) \times 10^3$	$(4.5 \pm 1.2) \times 10^3$	$(2.3 \pm 0.8) \times 10^3$
σ_C	0.07 ± 0.02	0.013 ± 0.005	ND	0.06 ± 0.04	0.07 ± 0.03	0.11 ± 0.04	ND
σ_{RC}	0.16 ± 0.04	0.02 ± 0.007	ND	0.17	0.11	0.15	ND

being approximately a factor of 5 higher than the corresponding affinities of the pyrimidine nucleotides (Tables 1 and 2). However, the values of parameters σ_C and σ_{RC}, characterizing cooperative interactions, are very similar for all examined cofactors (see the Discussion).

Role of the Phosphate Group and Ribose in Interactions of Nucleotide Cofactors with the RepA Helicase. In the case of most helicases, only nucleoside triphosphates can induce a high-affinity state of the protein for the ssDNA (*33*−*38*). Such an effect indicates that the γ phosphate is involved in allosteric interactions, extending beyond the nucleotide-binding site of the enzyme (*28*, *29*). To address the question as to what extent the specific structure of the ATP phosphate group affects the energetics of the nucleotide binding to the RepA helicase, we performed competition titration studies using various ATP analogues differing by the structure of the phosphate group.

Fluorescence titrations of the RepA helicase with TNP-ADP in the presence of two different adenosine triphosphates, β,γ-imodoadenosine-5′-triphosphate (AMP-PNP) and adenosine-5′-*O*-(3-thiotriphosphate) (ATPγS), in buffer T5 (at pH 7.6 and 10 °C), containing 10 mM NaCl and 5 mM $MgCl_2$, are shown in Figure 4a. Analogous titration of the RepA protein with TNP-ADP in the presence of 3 mM AMP−PCP is shown in Figure 4b. The selected concentrations of all ATP analogues are 3 mM. The solid lines in parts a and b Figure 4 are nonlinear least-square fits of the experimental titration curves according to the hexagon model of two competing, cooperatively binding ligands, using eqs 1−4 and the empirical function defined by eq 5. The obtained

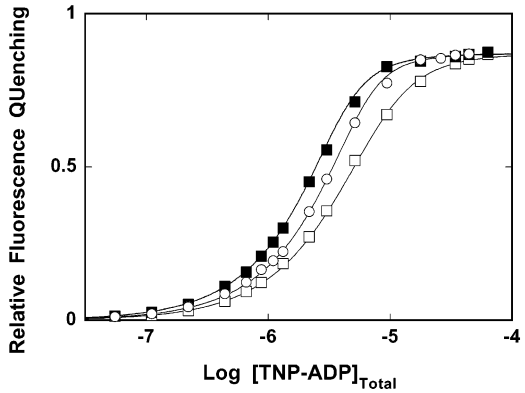

FIGURE 3: Fluorescence titration of the RepA helicase with TNP-ADP in buffer T5 (at pH 7.6 and 10 °C), containing 10 mM NaCl and 5 mM $MgCl_2$, in the absence (■) and presence of 3 mM GDP (□) or 3 mM TDP (○). The concentration of the RepA helicase is 1×10^{-6} M (hexamer). The solid lines are nonlinear least-square fits of the titration curves, according to the hexagon model for two competing ligands (eqs 2−4) and the empirical function defined by eq 5, using binding parameters for GDP and TDP included in Table 1. The intrinsic binding constant of the reference nucleotide, TNP-ADP, is $K = 1 \times 10^7$ M^{-1} and cooperativity parameter $\sigma = 0.3$.

binding parameters are included in Table 2. The values of intrinsic binding constants of all examined ATP analogues are lower than the values of the corresponding parameter obtained for ATP. This is particularly evident in the case of β,γ-methylenadenosine-5′-triphosphate (AMP-PCP), whose intrinsic binding constant is approximately 2 orders of magnitude lower than the intrinsic binding constant obtained for ATP. Notice, there is also a dramatic difference in the shape of the titration curves obtained in the presence of AMP-PNP and ATPγS, reflecting large differences in the values of the cooperativity parameter, σ_C, and σ_{RC} between both analogues (Figure 4a and Table 2). Thus, binding of AMP-PNP is characterized by a much lower value of σ_C, i.e., much stronger negative cooperative interactions than the binding of ATPγS; however, its value is similar to the values of σ_C obtained for ATP (Tables 1 and 2). Also, cooperative interactions between the reference nucleotide, TNP-ADP, and AMP-PNP, are characterized by $\sigma_{RC} = 0.02 \pm 0.007$, significantly lower than observed for ATPγS (Table 2) (see the Discussion).

To address the role of the sugar moiety in the binding of the nucleotide cofactors to the RepA helicase, we performed competition studies with dATP and dADP, using TNP-ADP as a reference ligand. Fluorescence titrations of the RepA helicase with the TNP-ADP in the presence of dATP or dADP in buffer T5 (at pH 7.6 and 10 °C), containing 10 mM NaCl and 5 mM $MgCl_2$, are shown in Figure 4c. The titration of RepA protein with TNP-ADP, in the absence of cofactors, is also included. The deoxyribonucleotide concentrations are 3 mM. The solid lines in Figure 4c are nonlinear least-square fits of the titration curves according to the hexagon model of two competing, cooperatively binding ligands (Figure 2), using eqs 1−4 and the empirical function defined by eq 5. The obtained binding parameters are included in Table 1.

The replacement of the ribose by deoxyribose has only a moderate effect on the nucleotide affinity, although different for ATP, as compared to the ADP cofactor. The intrinsic binding constant of dATP is by a factor of ∼2 lower, while the intrinsic binding constant for dADP is by a factor of ∼2 higher than the corresponding parameters obtained for ATP and ADP, respectively, indicating that the ribose 2′-OH group participates in the interactions in the binding site (Table 1). However, similar to ATP and ADP, the parameters σ_C and σ_{RC}, characterizing the cooperative interactions between the bound deoxyribose-adenosine cofactors and cooperative interactions with TNP-ADP, are lower for dATP as compared to dADP (Table 1).

Salt Effect on the ATP and ADP Analogues Binding to the RepA Helicase. The effect of salt on the energetics of the nucleotide cofactor binding to the RepA hexamer has been examined using TNP-ADP and TNP-ATP analogues. Fluorescence titrations of RepA protein with TNP-ADP, in

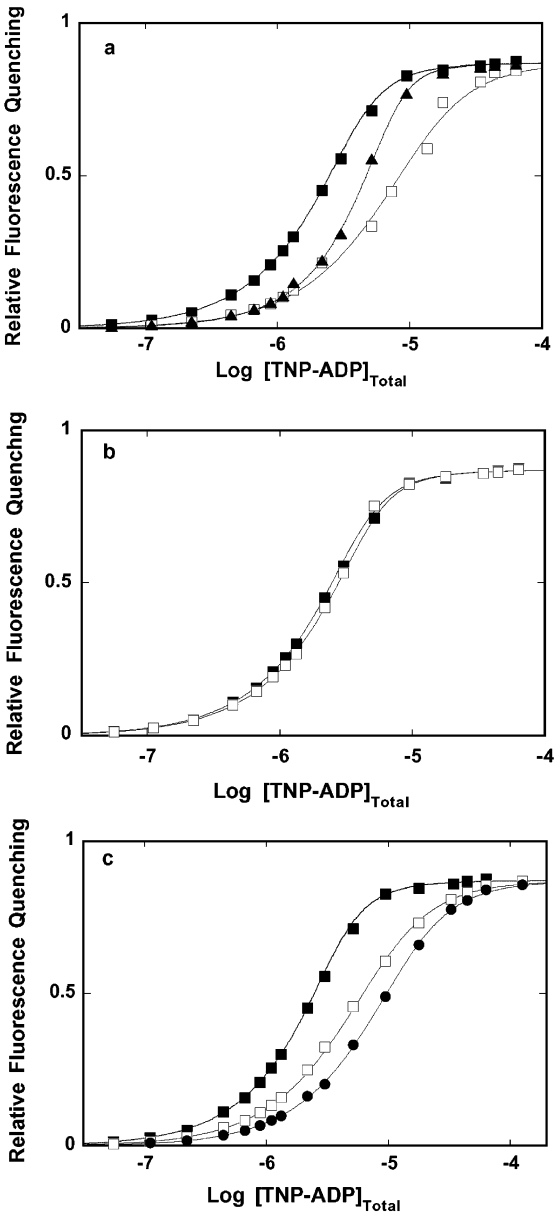

FIGURE 4: (a) Fluorescence titration of the RepA helicase with TNP-ADP in buffer T5 (at pH 7.6 and 10 °C), containing 10 mM NaCl and 5 mM $MgCl_2$, in the absence (■) and presence of 3 mM ATPγS (□) or 3 mM AMP-PNP (▲). The solid lines are nonlinear least-square fits of the titration curves, according to the hexagon model for two competing ligands (eqs 2−4) and the empirical function defined by eq 5, using binding parameters for ATPγS and AMP-PNP included in Table 2. (b) Fluorescence titration of the RepA helicase with TNP-ADP in buffer T5 (at pH 7.6 and 10 °C), containing 10 mM NaCl and 5 mM $MgCl_2$, in the absence (■) and presence (□) of 3 mM AMP-PCP. The solid lines are nonlinear least-square fits of the titration curves, according to the hexagon model for two competing ligands (eqs 2−4) and the empirical function defined by eq 5, using binding parameters for AMP-PCP included in Table 2. (c) Fluorescence titration of the RepA helicase with TNP-ADP in buffer T5 (at pH 7.6 and 10 °C), containing 10 mM NaCl and 5 mM $MgCl_2$, in the absence (■) and presence of 3 mM dATP (□) or 3 mM dADP (●). The solid lines are nonlinear least-square fits of the titration curves, according to the hexagon model for two competing ligands (eqs 2−4) and the empirical function defined by eq 5, using binding parameters for dATP and dADP included in Table 1. In a−c, the intrinsic 37 binding constant of the reference nucleotide, TNP-ADP, is $K = 1 \times 10^7$ M^{-1} and cooperativity parameter $\sigma = 0.3$; the concentration of the RepA helicase is 1×10^{-6} M (hexamer).

buffer T5 (at pH 7.6 and 10 °C), containing 1 mM $MgCl_2$ and different NaCl concentrations, are shown in Figure 5a. Analogous titrations in the presence of NaBr are shown in Figure 5b. As the salt concentration increases, the titration curves are shifted toward the higher TNP-ADP concentration range, indicating a decreasing macroscopic affinity of the nucleotide. However, the maximum fluorescence increase at saturation, ΔF_{max}, remains, within experimental accuracy, unaffected by the increasing [NaCl] or [NaBr], indicating that the structure of the protein−nucleotide complex, is minimally affected by the increased salt concentration. The solid lines in parts a and b of Figure 5 are nonlinear least-square fits of the spectroscopic binding curves according to the hexagon model (accompanying paper 1) and the empirical function defined by eq 5.

Figure 5c shows the dependence of the logarithm of the intrinsic binding constant of TNP-ADP, upon the logarithm of the NaCl concentration (log−log plot) (*40*, *41*). The plot is clearly nonlinear. At lower [NaCl], up to 100 mM, the plot is characterized by the slope $\partial \log K/\partial \log [NaCl] = -0.2 \pm 0.1$, an indication of a very modest effect of the salt on the cofactor binding. However, above [NaCl] ≈ 100 mM, the values of the intrinsic binding constant decrease dramatically with increasing NaCl concentrations in solution. The plot is linear, in the elevated salt concentration range, and characterized by the slope $\partial \log K/\partial \log [NaCl] = -1.9 \pm 0.3$, indicating that the net release of ∼2 ions accompanies the nucleoside diphosphate binding. The effect of the salt on the cooperative interactions between bound TNP-ADP molecules is different from the effect on its intrinsic affinity. The dependence of the logarithm of the cooperativity parameter, σ, upon the logarithm of the NaCl concentration is shown in Figure 5d. Although σ is virtually unchanged up to [NaCl] ≈ 100 mM, it slightly and steadily increases at higher salt concentrations, with the positive slope of the log−log plot, $\partial \log \sigma/\partial \log [NaCl] = 0.3 \pm 0.1$ (Figure 5d). The log−log plots for the binding of TNP-ADP to the RepA protein, in the presence of NaBr, are included in parts c and d of Figure 5. The data indicate a very similar behavior of the system in the presence of both salts, i.e., within experimental accuracy, the slopes $\partial \log K/\partial \log [NaBr] \approx \partial \log K/\partial \log [NaCl]$ and $\partial \log \sigma/\partial \log [NaBr] \approx \partial \log \sigma/\partial \log [NaCl]$, respectively. Moreover, not only are the slopes the same, but also the values of the intrinsic binding constant and cooperativity parameters are the same, in corresponding salt concentrations, independent of the type of anion in solution (see the Discussion).

Examination of the salt effect on the TNP-ATP binding to the RepA hexamer has been performed in an analogous way. A series of fluorescence titration curves of RepA protein with TNP-ADP, in buffer T5 (at pH 7.6 and 10 °C), containing 1 mM $MgCl_2$ and different NaCl concentrations, is shown in Figure 6a. Similar to the ADP analogue, the titration curves are significantly shifted to higher TNP-ATP concentrations, particularly at higher [NaCl], indicating a decrease in the macroscopic affinity of the cofactor. The dependence of the logarithm of the intrinsic binding constant of TNP-ATP, upon the logarithm of the NaCl concentration (log−log plot) is shown in Figure 6b. There are clearly two phases in the log−log plot. At low [NaCl], the plot is characterized by the slope $\partial \log K/\partial \log [NaCl] = -0.4 \pm 0.1$, slightly higher than observed for the TNP-ADP. On the

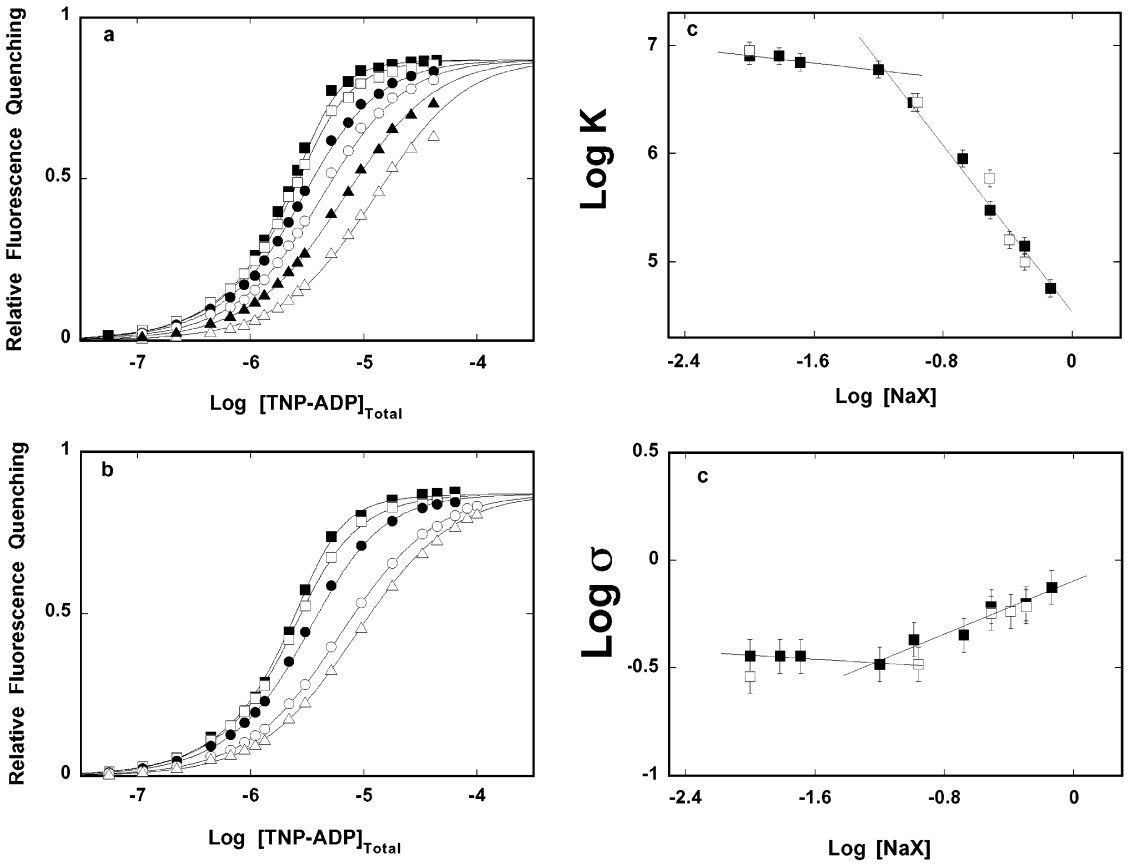

FIGURE 5: (a) Fluorescence titration of the RepA helicase with TNP-ADP in buffer T5 (at pH 7.6 and 10 °C), containing 1 mM $MgCl_2$, and different concentrations of NaCl, 10 mM (■), 103.2 mM (□), 209.6 mM (●), 309.6 mM (○), 509 mM (▲), and 730.8 mM (△). The solid lines are nonlinear least-square fits of the titration curves, according to the hexagon model and the empirical function defined by eq 5 (accompanying paper 1). (b) Fluorescence titration of the RepA helicase with TNP-ADP in buffer T5 (at pH 7.6 and 10 °C), containing 10 mM NaCl and 1 mM $MgCl_2$, containing different concentrations of NaBr, 10 mM (■), 109.2 mM (□), 308.8 mM (●), 408.4 mM (○), and 508 mM (△). The solid lines are nonlinear least-square fits of the titration curves, according to the hexagon model and the empirical function defined by eq 5 (accompanying paper 1). (c) Dependence of the logarithm of the intrinsic binding constant for the TNP-ADP binding to the RepA hexamer upon the logarithm of the NaCl (■) and NaBr (□) concentrations. The solid lines indicate the slopes of the linear parts of the plot in low and high salt concentration ranges (see the text for details). (d) Dependence of the logarithm of the cooperativity parameter, σ, for the TNP-ADP binding to the RepA hexamer upon the logarithm of the NaCl (■) and NaBr (□) concentrations. The solid lines indicate the slopes of the linear parts of the plot in low and high salt concentration ranges (see the text for details). In a−d, the concentration of the RepA helicase is 1×10^{-6} M (hexamer).

other hand, above [NaCl] ≈ 100 mM, the linear part of the plot is characterized by the slope $\partial \log K/\partial \log [NaCl] = -1.9 \pm 0.3$. Thus, the net release of ∼2 ions accompanies the intrinsic binding of the nucleoside triphosphate, the same value as observed for the intrinsic binding of TNP-ADP to the RepA helicase (see the Discussion).

The dependence of the logarithm of the cooperativity parameter, σ, for TNP-ATP binding to the RepA protein, upon the logarithm of [NaCl] is shown in Figure 6c. As observed in the case of the TNP-ADP, the values of σ do not significantly change in the low [NaCl] concentration range. However, above ∼50 mM NaCl, the log−log plot is characterized by a slight positive slope, $\partial \log \sigma/\partial \log [NaCl] = 0.17 \pm 0.1$ (Figure 6c). The log−log plots for the binding of TNP-ATP to the RepA protein, in the presence of NaBr, are also included in parts b and c of Figure 6. The data, within the experimental accuracy, superimpose on the log−log plots obtained in the presence of NaCl, indicating that, analogously to TNP-ADP, the intrinsic binding constants and cooperativity parameters, as well as the net number of released ions, accompanying the TNP-ATP binding, are independent of the type of anion in solution (see the Discussion).

Magnesium Effect on the Binding of Nucleotide Cofactors to the RepA Hexamer. Fluorescence titrations of RepA protein with TNP-ADP, at two different protein concentrations, in buffer T5 (at pH 7.6 and 10 °C), containing 10 mM NaCl and in the absence of $MgCl_2$, are shown in Figure 7a. The selected RepA hexamer concentrations are 1×10^{-6} and 1×10^{-5} M, respectively. The maximum fluorescence quenching observed at saturation, $\Delta F_{max} = 0.8 \pm 0.03$; i.e., it is lower than observed in the presence of Mg^{2+} (0.87 ± 0.03) (see below). The solid lines in Figure 7a are nonlinear least-square fits of the spectroscopic titration curves according to the hexagon model and using the empirical function, which, in this case, is defined by a third-degree polynomial (data not shown)

$$\Delta F_{obs} = 3.5941 \times 10^{1}(\sum \Theta_i) - 6.5685 \times 10^{2}(\sum \Theta_i)^2 - 4.7197 \times 10^{3}(\sum \Theta_i)^3 \quad (6)$$

The obtained intrinsic binding constant $K = (5.0 \pm 1) \times 10^4\ M^{-1}$, and the cooperative interaction parameter, $\sigma = 1.24$

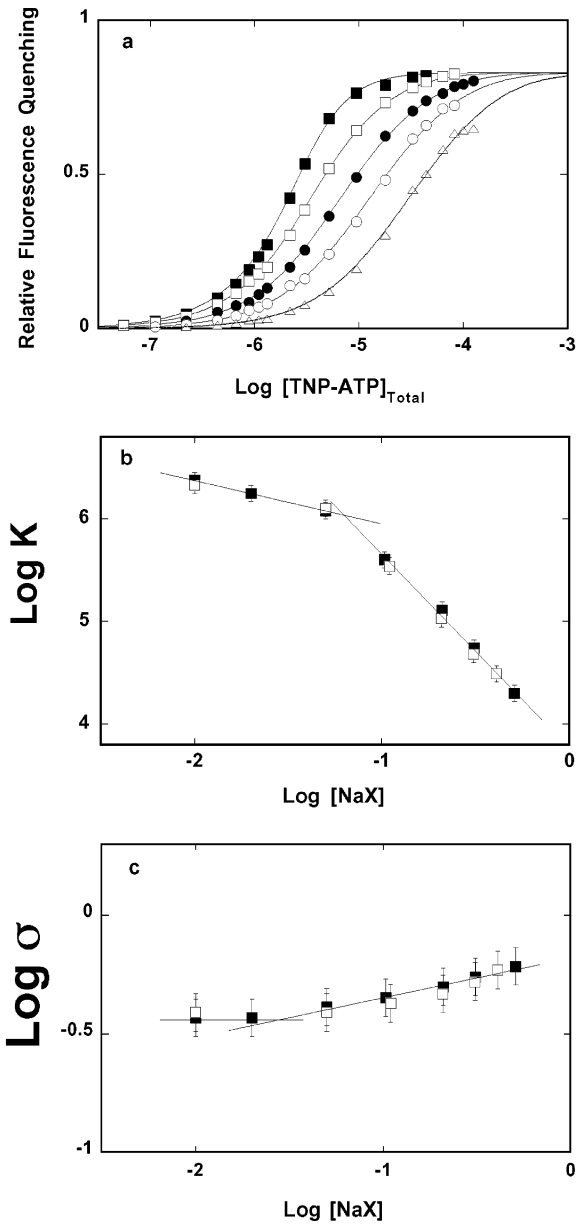

FIGURE 6: (a) Fluorescence titration of the RepA helicase with TNP-ATP in buffer T5 (at pH 7.6 and 10 °C), containing 1 mM $MgCl_2$, and different concentrations of NaCl, 10 mM (■), 103.2 mM (□), 209.6 mM (●), 309.3 mM (○), and 509 mM (△). The solid lines are nonlinear least-square fits of the titration curves, according to the hexagon model and the empirical function defined by eq 5 (accompanying paper 1). (b) Dependence of the logarithm of the intrinsic binding constant for the TNP-ATP binding to the RepA hexamer upon the logarithm of the NaCl (■) and NaBr (□) concentrations. The solid lines indicate the slopes of the linear parts of the plot in low and high salt concentration ranges (see the text for details). (c) Dependence of the logarithm of the cooperativity parameter, σ, for the TNP-ATP binding to the RepA hexamer upon the logarithm of the NaCl (■) and NaBr (□) concentrations. The solid lines indicate the slopes of the linear parts of the plot in low and high salt concentration ranges (see the text for details). In a−c, the concentration of the RepA helicase is 1×10^{-6} M (hexamer).

± 0.25. Thus, in the absence of magnesium, the intrinsic affinity of the ADP analogue decreases dramatically, by approximately 2 orders of magnitude. Moreover, the negative cooperative interactions between bound cofactor molecules strongly diminish, and the binding process becomes noncooperative or characterized by a slightly positive cooperativity. Fluorescence titrations of the RepA protein with TNP-ADP in buffer T5 (at pH 7.6 and 10 °C), containing 10 mM NaCl and selected concentration of $MgCl_2$, are shown in Figure 7b. As the magnesium concentration increases, the titration curves are shifted toward lower TNP-ADP concentrations, indicating a strong increase of the macroscopic affinity of the cofactor. Such behavior indicates that, instead of release, there is an uptake of ions accompanying the binding of the nucleotide cofactor to the RepA hexamer. Also, even at a very low [$MgCl_2$] (5×10^{-5} M), the value of the maximum fluorescence quenching at saturation, ΔF_{max}, has already the same value as observed at the high magnesium concentrations.

The dependence of the logarithm of the intrinsic binding constant, K, of TNP-ADP upon the logarithm of the $MgCl_2$ concentration is shown in Figure 7c. The character of the plot is very different from the analogous log−log plots obtained for the NaCl and NaBr (Figure 5c). There are clearly two binding processes, marked by two plateaus. Because of the high affinity, the first binding process could not be quantitatively accessed (see below). In the high-affinity-binding phase, the intrinsic binding constant of TNP-ADP increases from $(5.0 \pm 1) \times 10^4$ M^{-1} to $(8.5 \pm 1.3) \times 10^5$ M^{-1}, at the intermediate plateau, i.e., by more than an order of magnitude. The second binding phase occurs at a much higher [$MgCl_2$] and induces a further increase of the intrinsic binding constant by an order of magnitude, with $K = (1 \pm 0.2) \times 10^7$ M^{-1} in the final plateau. Further increase of the [$MgCl_2$] above 5 mM results in only a slight decrease of the affinity of the cofactor, suggesting an additional unresolved, weak affinity Mg^{2+}-binding process.

There are two fundamental aspects of the data shown in Figure 7c. First, the observed ion-binding process must exclusively include magnesium cations, because the salt effect on the cofactor binding, discussed above, does not indicate any anion participation in the cofactor binding, particularly in the low salt concentration range. Second, the two resolved binding phases are separated by at least 3 orders of magnitude in affinity, indicating that very different magnesium-binding sites are involved. The high-affinity binding phase occurs in the micromolar concentration range of magnesium. Notice, in the examined solution conditions, the nucleotide cofactor binds a magnesium cation with the affinity of $\sim 10^6$ M^{-1} (*42*). The low-affinity phase is in the millimolar concentration range of magnesium, and it must involve binding of Mg^{2+} to the protein. Thus, the simplest interpretation of the experimental behavior is that one observes the effect of the magnesium binding to the nucleotide cofactor and to the RepA protein on the intrinsic affinity of the nucleotide binding to the helicase.

In this simplest interpretation of the observed effect of magnesium on the overall intrinsic binding process of the ADP analogue binding to the RepA hexamer, the following partial binding equilibria must be considered. Binding of a magnesium cation to the free nucleotide cofactor, N_0, forming the cofactor−Mg^{2+} complex, N_1, characterized by the binding constant K_N; binding of j magnesium cations to the free RepA protein, P_0, forming RepA protein−Mg^{2+}_j complex, P_1, characterized by the binding constant K_{M1}; binding of the free cofactor and its magnesium complex to the free RepA protein, forming P_{00} and P_{01} complexes, characterized by the binding constants K_{00} and K_{01}, respectively; and binding of

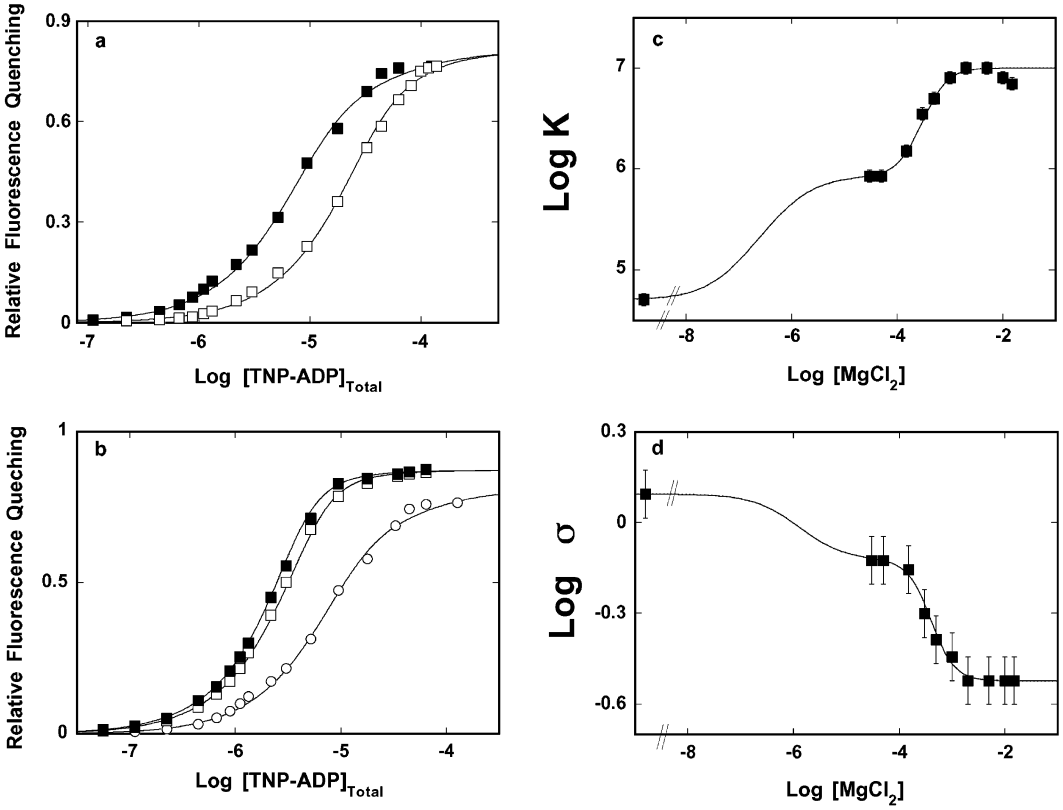

FIGURE 7: (a) Fluorescence titration of the RepA helicase with TNP-ADP in buffer T5 (at pH 7.6 and 10 °C), containing 10 mM NaCl and no magnesium, at different RepA protein concentrations, (■) 1×10^{-6} M and (□) 1×10^{-5} M (hexamer). The solid lines are nonlinear least-square fits of the titration curves, according to the hexagon model (accompanying paper 1), using a single set of binding parameters with the intrinsic binding constant $K = 5.03 \times 10^4$ M^{-1}, cooperativity parameter $\sigma = 1.244$, and the empirical function defined by eq 6. (b) Fluorescence titration of the RepA helicase with TNP-ADP in buffer T5 (at pH 7.6 and 10 °C), containing 10 mM NaCl and different $MgCl_2$ concentrations, (■) 0, (□) 5×10^{-5} M, and (○) 5 mM. The solid lines are nonlinear least-square fits of the titration curves, according to the hexagon model (accompanying paper 1), using the intrinsic binding constant $K = 5.03 \times 10^4$ M^{-1}, $\sigma = 1.244$ (■); $K = 8.5 \times 10^{-5}$ M^{-1}, $\sigma = 0.75$ (□); and $K = 1 \times 10^7$ M^{-1}, $\sigma = 0.3$ (○), and the empirical function defined by eq 6. (c) Dependence of the logarithm of the intrinsic binding constant for the TNP-ADP binding to the RepA hexamer upon the logarithm of the $MgCl_2$ concentration (■). The solid line is the nonlinear least-square fit of the experimental curve to eq 8b, with $K_{M1} = (1.8 \pm 0.3) \times 10^3$ M^{-1} (see the text for details). (d) Dependence of the logarithm of the cooperativity parameter, σ, for the TNP-ADP binding to the RepA hexamer upon the logarithm of the $MgCl_2$ concentration (■). The solid line is the nonlinear least-square fit of the experimental curve to eq 9, with $K_{M2} = (3.1 \pm 1) \times 10^3$ M^{-1} (see the text for details).

the free cofactor and its magnesium complex to the magnesium-saturated RepA protein, forming P_{10} and P_{11} complexes, characterized by the binding constants K_{10} and K_{11}, respectively. These equilibria are defined as

$$N_0 + Mg^{2+} \leftrightarrow N_1 \quad (7a)$$

$$P_0 + j\,Mg^{2+} \leftrightarrow P_1 \quad (7b)$$

$$P_0 + N_0 \leftrightarrow P_{00} \quad (7c)$$

$$P_0 + N_1 \leftrightarrow P_{01} \quad (7d)$$

$$P_1 + N_0 \leftrightarrow P_{10} \quad (7e)$$

$$P_1 + N_1 \leftrightarrow P_{11} \quad (7f)$$

The overall intrinsic binding constant, K, at a given magnesium concentration, is then defined as

$$K = \frac{K_{00} + K_{01}K_N[Mg] + K_{10}(K_{M1}[Mg])^j + K_{11}K_N(K_{M1}[Mg])^j}{(1 + K_N[Mg])[1 + (K_{M1}[Mg])^j]} \quad (8a)$$

Although there are seven parameters, K_{00}, K_{01}, K_N, K_{10}, K_{M1}, K_{11}, and j in eq 8a, most of them can be obtained independently. The value of $K_{00} = (5.0 \pm 1) \times 10^4$ M^{-1} is known from independent titration in the absence of magnesium (Figure 7a). The value of $K_{01} = (8.5 \pm 1.3) \times 10^5$ M^{-1} is known from the intermediate plateau in Figure 7c, and $K_{11} = (1.0 \pm 0.2) \times 10^7$ M^{-1} is known from independent fluorescence titrations in saturating concentrations of $MgCl_2$, at the final plateau in Figure 7c. The log−log plot of the low-affinity phase provides the minimum value of $j = 2 \pm 0.3$, independent of any binding model (data not shown). Moreover, because of the large difference in the affinities between the two binding phases, the nucleotide cofactor is always saturated with Mg^{2+} prior to the cation binding to the protein and the equilibrium, defined by eq 7e, does not

affect the overall intrinsic affinity of the nucleotide cofactor to any detectable extent. Therefore, eq 8a simplifies to

$$K = \frac{K_{00} + K_{01}K_N[Mg] + K_{11}K_N(K_{M1}[Mg])^j}{(1 + K_N[Mg])[1 + (K_{M1}[Mg])^j]} \quad (8b)$$

Thus, there are only two unknown parameters, K_N and K_{M1}, in eq 8b that have to be determined, although only a minimum value of K_N can be obtained, because of the high affinity of the first binding phase (see above). The solid line in Figure 7c is the computer fit of the experimental curve, using K_{M1} as a fitting parameter, which provides $K_{M1} = (1.8 \pm 0.3) \times 10^3\ M^{-1}$, with the minimum value of $K_N \approx 10^6\ M^{-1}$ (*42*). Thus, intrinsic binding of the ADP analogue to the RepA nucleotide-binding site is accompanied by the binding of ~2 magnesium cations, whose affinity is characterized by an association constant in the range of $\sim 10^3\ M^{-1}$.

The dependence of the logarithm of the cooperative interaction parameter, σ, for the TNP-ADP binding to the RepA hexamer, upon the $MgCl_2$ concentration is shown in Figure 7d. Unlike the intrinsic binding constant, the values of σ decrease with the increasing concentration of magnesium, from 1.24 ± 0.25, in the absence of Mg^{2+}, to 0.30 ± 0.06, at a high concentration range of $MgCl_2$. The further increase of the [$MgCl_2$], above 2 mM, does not affect the cooperative interactions. However, similar to the behavior of the intrinsic binding constant, there are two binding phases of the cation, with two plateaus in the plot. As discussed above for the intrinsic affinity, such behavior of σ indicates that cooperative interactions between the bound ADP analogue molecules are accompanied by specific magnesium-binding processes. Analogously to the intrinsic binding constant (eq 8b), the observed values of the cooperativity parameter, σ_{obs}, at a given magnesium concentration, can be then defined as

$$\sigma_{obs} = \frac{\sigma_{00} + \sigma_{01}K_N[Mg] + \sigma_{11}K_N(K_{M2}[Mg])^p}{(1 + K_N[Mg])[1 + (K_{M2}[Mg])^p]} \quad (9)$$

where σ_{00} and σ_{01} are the cooperativity parameters characterizing binding of the free TNP-ADP and the TNP-ADP−Mg^{2+} complex to magnesium-free RepA protein, σ_{11} is the cooperativity parameter characterizing the binding of the TNP-ADP−Mg^{2+} complex to RepA protein saturated with magnesium, p is the number of Mg^{2+} cations that bind to the helicase and accompany the formation of cooperative interactions, and K_{M2} is the binding constant characterizing the binding of Mg^{2+} cations to the enzyme. Notice, in general, that the values of p and K_{M2} do not have to be the same as j and K_{M1} characterizing the Mg^{2+} effect on the intrinsic affinity of the analogue (eq 8b).

Because, as in the case of the intrinsic binding constant (see above), $\sigma_{00} = 1.24 \pm 0.25$, $\sigma_{01} = 0.75 \pm 0.15$, $\sigma_{01} = 0.30 \pm 0.06$, and $p = 2.0 \pm 0.4$ can be determined independently, as described above for the intrinsic binding process, only two parameters, K_N, and K_{M2}, are unknown. The solid line in Figure 8d is the computer fit of the experimental plot that provide $K_{M2} = (3.1 \pm 1) \times 10^3\ M^{-1}$ and the minimum value of $K_N = 1 \times 10^6\ M^{-1}$ (*42*). Thus, the transition from a slightly positive cooperative binding of the TNP-ADP, to the binding process characterized by negative cooperative interactions, is accompanied by association of ~2 magnesium cations to the RepA helicase. Moreover, the affinity of these magnesium-binding sites is, within experimental accuracy, the same as the affinity of the Mg^{2+} sites that affect the intrinsic binding process of the ADP analogue (see the Discussion).

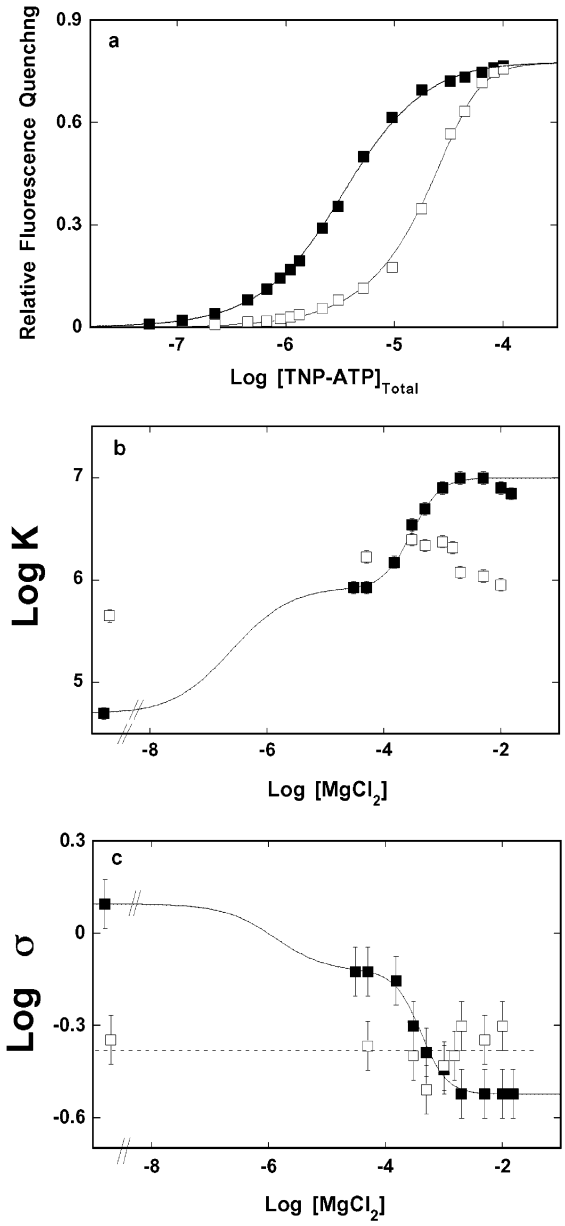

FIGURE 8: (a) Fluorescence titration of the RepA helicase with TNP-ATP in buffer T5 (at pH 7.6 and 10 °C), containing 10 mM NaCl and no magnesium, at different RepA protein concentrations, (■) 1×10^{-6} M and (□) 1×10^{-5} M (hexamer). The solid lines are nonlinear least-square fits of the titration curves, according to the hexagon model (accompanying paper 1), using a single set of binding parameters with the intrinsic binding constant $K = 4.5 \times 10^4\ M^{-1}$, cooperativity parameter $\sigma = 0.45$, and the empirical function defined by eq 10. (b) Dependence of the logarithm of the intrinsic binding constant for the TNP-ATP binding to the RepA hexamer upon the logarithm of the $MgCl_2$ concentration (□) superimposed on the analogous plot obtained for the TNP-ADP (Figure 8c). (c) Dependence of the logarithm of the cooperativity parameter, σ, for the TNP-ADP binding to the RepA hexamer upon the logarithm of the $MgCl_2$ concentration (□) superimposed on the analogous plot obtained for TNP-ADP (Figure 7d).

Analogous analyses of the magnesium effect have been performed for the ATP analogue, TNP-ATP, binding to the RepA hexamer. Fluorescence titrations of RepA protein with TNP-ATP, at two different protein concentrations [1×10^{-6} and 1×10^{-5} M (hexamer)], in buffer T5 (at pH 7.6 and 10 °C), containing 10 mM NaCl and in the absence of $MgCl_2$, are shown in Figure 8a. Similar to TNP-ADP, the maximum fluorescence quenching observed at saturation, $\Delta F_{max} = 0.78 \pm 0.02$; i.e., it is lower than observed in the presence of magnesium (0.83 ± 0.02) (accompanying paper 1). The dependence of the fluorescence quenching, ΔF_{obs}, upon the average degree of binding, $\sum\Theta_i$, of TNP-ATP on the RepA hexamer is shown in Figure 8b. The plot is nonlinear and described by the empirical function, defined by the second-degree polynomial, as

$$\Delta F_{obs} = 2.5108 \times 10^{1}(\sum\Theta_i) - 2.0255 \times 10^{2}(\sum\Theta_i)^2 \quad (10)$$

The solid lines in Figure 8a are the nonlinear least-square fits of the titration curves of the TNP-ATP binding to the RepA hexamer, according to the hexagon model and using the determined empirical function (eq 10), with a single set of binding parameters that provide the intrinsic binding constant $K = (4.5 \pm 0.5) \times 10^5$ M^{-1} and $\sigma = 0.45 \pm 0.09$. Thus, the absence of Mg^{2+} has a different effect on the ATP than on the ADP analogue. Instead of ~2 orders of magnitude decrease in the intrinsic affinity, the intrinsic binding constant of TNP-ATP is lower only by a factor of ~5, as compared to the value observed in the presence of Mg^{2+} (accompanying paper 1). Moreover, binding of TNP-ATP to the protein in the absence of Mg^{2+} is characterized by negative cooperativity, virtually the same as determined in the presence of Mg^{2+}.

The dependence of the logarithm of the intrinsic binding constant, K, of TNP-ATP upon the logarithm of the $MgCl_2$ concentration is shown in Figure 8b. For comparison, the data are superimposed on the same plot obtained for the ADP analogue (Figure 7c). Unlike the TNP-ADP, the intermediate plateau is absent and, as a result, the plot does not exhibit clear and different binding phases. Nevertheless, a further increase of the $MgCl_2$ concentration, above 2 mM, results in a slight and gradual decrease of the intrinsic affinity of the cofactor, suggesting the presence of another weak binding process of magnesium. The dependence of the cooperative interaction parameter, σ, upon $MgCl_2$ concentration is shown in Figure 8c together with the data obtained for TNP-ADP. The difference between the ATP and ADP analogues are even more striking. Within the experimental accuracy, the cooperativity parameter σ, determined for TNP-ATP, is not affected by the changes in the magnesium cation concentrations. In other words, the binding of the ATP analogue is always characterized by negative cooperativity (see the Discussion).

DISCUSSION

ATP Binds to the RepA Hexamer with Higher Intrinsic Affinity than ADP and Inorganic Phosphate. A direct, quantitative estimate of the ATP intrinsic affinity for the nucleotide-binding site is not currently available for any hexameric helicase. The fact that, in the solution conditions applied in our studies, the RepA helicase does not hydrolyze ATP to any detectable extent, on the time scale of the binding experiments, allowed us to characterize, for the first time, the intrinsic affinities of ATP, ADP, and inorganic phosphate to a hexameric helicase. The intrinsic binding constant of ATP is by a factor of ~10 and ~1000 higher than the value observed for ADP and PO_4^-. Such order of affinities of ATP and its hydrolysis products is expected for an enzyme that performs free-energy transduction because the strong ATP binding, as compared to ADP and PO_4^-, may allow the enzyme to hydrolyze ATP in the active site with a very low change of the free energy, as proposed for myosin (*43*, *44*). However, the observed difference in affinity is not high enough to enable the RepA helicase to efficiently store the free energy of ATP hydrolysis (*43*, *44*). In the case of the *E. coli* DnaB hexamer, an estimate of the ATP binding energy is very difficult to obtain because of the very potent ATPase activity of the enzyme, even in the absence of the nucleic acid (*45*). The obtained data indicate that the ATP affinity for the DnaB helicase is even lower than the affinity of ADP and both ATP and ADP bind with approximately 3 orders of magnitude higher affinity than the PO_4^- group (*21*, *30*, *45*). However, similar to myosin, the ATP hydrolysis in the active site of the DnaB helicase is characterized by a very low equilibrium constant (~2); i.e., the ATP hydrolysis in the active site releases much less free energy than the same reaction in solution. In other words, the mechanism of storing the energy of ATP hydrolysis by both the DnaB and RepA hexamers, which can be used to perform the dsDNA unwinding and mechanical work of translocation along the DNA lattice, may be, in some aspects, different from the mechanism proposed for myosin. Recall that the ATPase activities of both enzymes are additionally activated in the complex with the ssDNA, albeit the energetics of ATP, ADP, and inorganic phosphate binding to a helicase, bound to the DNA, is not currently known for any helicase. As we proposed before, it is possible that a hexameric helicase acquires free-energy-transducing capabilities, similar to myosin, when associated with the ssDNA, thus forming a "holoenzyme" (*21*). The results on ATP, ADP, and inorganic phosphate binding, now available for two replicative hexameric helicases, strongly suggest such a possibility.

ATP Binding to the RepA Hexamer Is Characterized by a Significantly Stronger Negative Cooperativity Than ADP. Significant preference for ATP by the nucleotide-binding site of the RepA helicase indicates that the enzyme will be, most of the time, in a state of high affinity toward the ssDNA, ensuring very efficient binding. However, cooperative interactions between the bound ATP molecules are characterized by the cooperativity parameter, $\sigma_C \approx 0.003$, which is a factor of ~57 lower than $\sigma_C \approx 0.17$ obtained for ADP (Table 1). Thus, binding of ATP to the RepA hexamer is characterized by much stronger negative cooperative interactions than ADP. Moreover, cooperative interactions between ATP and ADP analogues are characterized by $\sigma_{RC} \approx 0.11$, much more favorable than between triphosphate molecules alone.

There are two profound implications of these data. First, the obtained binding parameters for ATP (Table 1) indicate that, predominantly, only three ATP molecules associate with the RepA hexamer up to [ATP] ≈ 5−10 mM, i.e., in the physiological concentration range of the cofactor (*44*). In other words, in the physiological concentration range of ATP,

only three nucleotide-binding sites of the RepA hexamer are saturated with ATP. In this context, we could determine that all six nucleotide-binding sites of the RepA hexamer can engage in interactions with the nucleotide cofactor only because of the much higher affinity of the TNP and MANT analogues for the binding sites of the enzyme than the affinities of unmodified nucleotides and significantly lower negative cooperativity characterizing the binding of the analogues (accompanying paper 1).

Second, as a result of strong negative cooperative interactions between bound ATP molecules, only every other site of the hexamer will be bound with ATP. However, because all nucleotide-binding sites can engage in interactions with the cofactor, the data indicate that the selection of the subunits occurs randomly, during the ATP-binding process (accompanying paper 1). Moreover, because the negative cooperative interactions between the ATP and ADP ($\sigma_{RC} \approx 0.11$) are significantly weaker than between ATP molecules, in the mixture of the both cofactors, at millimolar concentrations, the nucleotide-binding sites of the RepA hexamer will be alternatively saturated with ATP and ADP and such a complex. Recall, only ATP and ATP analogues induce the high ssDNA-affinity state of both the DnaB and the RepA hexamer (*6*, *26*, *27*). The mechanism of ssDNA binding to the RepA hexamer is still unknown. However, the obtained data strongly suggest that only three subunits of the RepA hexamer, saturated with a nucleoside triphosphate may serve as the initial binding sites for the nucleic acid. This behavior of the RepA hexamer is very different from the *E. coli* DnaB hexamer, where initially all six subunits of the hexamer, saturated with the nucleoside triphosphate, can serve as the binding site for the ssDNA (*21*−*23*, *30*).

Both Negative Cooperative Interactions and Intrinsic Affinity Are Predominantly Affected by the Structure of the Phosphate Group. The effect of the structure of the phosphate group on the intrinsic affinity of ATP analogues and the negative cooperative interactions is dramatic (Table 2). The value of σ_C is by a factor of ∼4 and ∼23 higher for AMP-PNP and ATPγS than observed for ATP. Also, the structure of the triphosphate group affects the cooperative interactions between ATP and ADP analogues, simultaneously bound to the RepA hexamer, as expressed by the different values of σ_{RC} (Table 2). However, the binding of TNP-ATP, where the modification is located on the ribose, as well as dATP, to the RepA hexamer is characterized by much weaker negative cooperative interactions than observed for ATP (accompanying paper 1 and Tables 1 and 2). Notice also, that contrary to the nucleoside triphosphates, the values of σ_C and σ_{RC}, for nucleoside diphosphates, are very similar, independent of the type of base and the presence or absence of a chemical modification on the ribose (accompanying paper 1 and Table 2).

Such behavior indicates that, in the case of the nucleoside triphosphates, the negative cooperative interactions are predominantly induced through the specific interactions of the phosphate groups, particularly γ phosphate, with the protein matrix and a complex interplay between the γ phosphate and the ribose-binding regions of the nucleotide-binding site. This conclusion is supported by the fact that the salt effect on the cooperative interactions does not indicate the presence of a simple ion exchange between the phosphate group and ions bound to the protein (see below). The structure of the phosphate group has also a pronounced effect on the intrinsic affinities of ATP analogues, with the affinity of AMP-PCP being approximately a factor of 200 lower than the intrinsic affinity of ATP. These data provide an indication that the major part of the free energy of binding of nucleotide cofactors is generated through the phosphate binding. It is interesting that binding of the inorganic phosphate is characterized by the cooperativity parameters similar to ADP (Table 1). These data and the efficient competition of PO_4^- with the ADP analogue for the nucleotide-binding site strongly suggest that the inorganic phosphate binds to the same site as the second phosphate of nucleoside diphosphate.

RepA Helicase Exhibits Preference for Purine Nucleotides. The intrinsic binding constants for the ADP and GDP are a factor of ∼5 higher than the analogous intrinsic affinity of TDP and CDP (Table 2). Thus, similar to the DnaB hexamer, the RepA helicase shows a preference for the purine nucleotide cofactors, as compared to the pyrimidine cofactors. However, with the exception of UDP, the type of the base affects the intrinsic affinity to a much weaker extent than the phosphate group (see above). The lack of an effect of the type of base on cooperative interactions is rather striking. As mentioned above, it reinforces the conclusion that the cooperative interactions are mainly induced by the interactions of the phosphate group and ribose with the protein. Current data indicate that the RepA helicase can hydrolyze NTPs independently of the type of the base, although with different specific activities (*8*). On the other hand, the equilibrium studies, reported here, point to an important caveat in such estimates. To quantitatively compare different NTPase activities, the saturation of the nucleotide-binding sites of the enzyme has to be the same for all examined cofactors, rather than the use of the same concentration of the nucleotides. Otherwise, instead of different specific activities, the activities of different numbers of active sites, engaged in NTP hydrolysis, are observed.

Salt Effect on the Nucleotide Cofactor Binding to the RepA Hexamer Indicates a Different Nature of Intrinsic and Cooperative Interactions. The salt effect provides additional information about the nature of interactions in the nucleotide-binding site of the RepA helicase. The same net numbers of released ions (∼2) accompany the intrinsic binding of ATP and ADP analogue, i.e., the net number of ions released, is not affected by the presence of the additional γ-phosphate group in the case of the ATP analogue (Figures 5c and 6b). Moreover, there is not anion release in the intrinsic binding of both cofactors, in the examined salt concentration range, strongly suggesting that only cations participate in the ion-exchange process (*40*, *41*). Such an observation indicates that instead of simple competition between the phosphate groups and anions, the intrinsic binding of the cofactors induces a specific cation release from the protein. The nonlinear character of the log−log plots for both ATP and ADP analogues would result from the fact that one observes binding of cations to their binding sites on the protein with the binding constant, $\sim 20\ M^{-1}$. The salt effect on cooperative interactions of both, the ATP and ADP analogue is very different from the analogous effect on the intrinsic binding process. It is much less pronounced, and at a high salt concentration, the log−log plots become positive, instead of negative, indicating some uptake of ions. These data

provide clear thermodynamic evidence that interactions of a very different nature are involved in the intrinsic binding, as compared to the cooperative interactions. The effect of Mg^{2+} on intrinsic binding and cooperative interactions of the ATP and ADP analogues further reinforces that conclusion (see below).

Binding of Magnesium Cations to the RepA Helicase Predominantly Controls the Intrinsic Affinity and Negative Cooperative Interactions of the ADP Binding to the Enzyme. The results described above clearly show that the RepA hexamer can bind ATP and ADP analogues in the absence of magnesium (Figures 7a and 8a). Although the Mg^{2+} effect on the cofactor binding to the analogous DnaB hexamer could not be examined, because the hexameric structure of this protein disintegrates in the absence of Mg^{2+}, binding of nucleotides, in the absence of Mg^{2+}, was observed in the case of another hexameric helicase, the bacteriophage T7 enzyme (*13*).

The magnesium effect on cofactor binding to the RepA hexamer is complex and very different from the salt effect, discussed in the previous section. A net uptake of Mg^{2+} cations, not a release, accompanies the formation of the intrinsic and cooperative interactions. Moreover, there is a dramatic difference between the effects of magnesium on the binding of ADP versus ATP analogue. In the case of the ADP analogue, there are clearly two phases of the magnesium uptake in the intrinsic binding process, while there are not such clear phases of cation uptake in the case of the ATP analogue (Figures 7c and 8b). In the absence of Mg^{2+}, the intrinsic affinity of the ADP analogue is decreased by a factor of $\sim$200, from $\sim 1 \times 10^7$ to $\sim 5 \times 10^4$ M^{-1}, as compared to the decrease of only by a factor of $\sim$5 in the case of the ATP analogue (Figure 8b). The ADP$-Mg^{2+}$ complex exhibits an intrinsic affinity that is higher by approximately 1 order of magnitude than the free nucleotide ($\sim 8.5 \times 10^5$ M^{-1}), while the affinity of the ATP$-Mg^{2+}$ complex is only slightly different from the free ATP analogue. Moreover, further increase of the magnesium concentration results in the appearance of the second phase of the cation binding and a further increase of the TNP-ADP intrinsic affinity, but it has even a diminishing effect on the intrinsic affinity of the TNP-ATP binding, possibly, indicating another cation-binding process. Because, in our solution conditions, the nucleotides are already saturated with magnesium in the millimolar Mg^{2+} concentration range, the presence of the second cation-binding phase indicates the presence of specific binding of Mg^{2+} cations to the protein, with a binding constant of $\sim 10^3$ M^{-1}. In fact, the data indicate that the binding of a minimum of 2 magnesium cations to the protein accompanies the intrinsic binding of the ADP analogue to the RepA hexamer.

A similar dramatic difference between the effects of magnesium on the ADP versus ATP analogue is observed for the cooperative interactions. Unlike the intrinsic affinity, the cooperative interaction parameter, σ, of the ADP analogue decreases with the increase of the magnesium concentration (Figure 7d). However, the process encompasses the same two cation-binding phases, and binding of two Mg^{2+} cations accompanies the formation of the cooperative interactions. This similarity indicates that the effect of magnesium binding to the same binding sites, i.e., to the nucleotide and protein, is observed. In the absence of Mg^{2+}, the ADP analogue binds noncooperatively to the RepA hexamer or with even slight positive cooperativity with $\sigma \approx 1.2$. The binding of the ADP$-Mg^{2+}$ complex is characterized by $\sigma \approx 0.7$, while at saturating concentrations of magnesium, $\sigma \approx 0.3$; i.e., when the Mg^{2+}-binding sites on the protein are saturated with the cations, the binding of the ADP analogue is characterized by significant, negative cooperative interactions. Contrary to the ADP analogue, the cooperative interactions of the TNP-ATP analogue are not, within experimental accuracy, affected by magnesium.

These results are very surprising. Rather an opposite effect, particularly in the case of intrinsic affinity, would be expected, because the magnesium cations are necessary for the NTPase activity of the enzyme. First, as we discussed above, these data indicate that the intrinsic affinity of NTP for the nucleotide-binding site of the RepA hexamer is predominantly determined by the interactions between the phosphate groups and ribose with the protein, and it is not mediated by the magnesium cations, although the structure of the complex is different, as indicated by the lower fluorescence quenching observed in the absence of Mg^{2+}. Because the catalytic activity of the enzyme requires a millimolar magnesium concentration, the data also indicate that magnesium effect on the binding of NTP cofactors is largely separated from the catalysis. Such separation strongly suggests that the magnesium cations have a dual function in NTP cofactor binding to the enzyme. At low [Mg^{2+}], the binding of nucleoside triphosphate is favored over NDP, leading to the increased ssDNA affinity, because the nucleic acid has lower affinity for the enzyme$-$NDP than the enzyme$-$NTP complex. At higher magnesium concentrations, NTP binds weaker than NDP and the helicase subunits can now exist in alternating low- and high-affinity states for the ssDNA that facilitate the efficient catalysis of the dsDNA unwinding (*15*$-$*17*). In other words, binding of Mg^{2+} cations to the helicase would affect the distribution of the high- and low-affinity binding sites of the ssDNA (parts a and b of Figure 9). Moreover, magnesium binding affects predominantly the intrinsic affinity and cooperative interactions of the product of the NTP hydrolysis, i.e., NDP, and the structure of the formed complex. When the intrinsic affinity of NDP is affected, magnesium binding to the protein would control the efficiency of the free-energy transduction of the enzyme.

ACKNOWLEDGMENT

We thank Betty Sordahl for reading the manuscript.

REFERENCES

1. De Gaaf, J., Crossa, J., H., Heffron, F., and Falkow, S. (1978) Replication of the nonconjugative plasmid RSF1010 in *Escherichia coli* K-12, *J. Bacteriol. 134*, 1117$-$1122.
2. Guerry, P., van Embden, J., and Falkow, S. (1974) Molecular nature of two nonconjugative plasmids carrying drug resistance genes, *J. Bacteriol. 117*, 987$-$997.
3. Scherzinger, E., Ziegelin, G., Barcena, M., Carazo, J. M., Lurz, R., and Lanka, E. (1997) The RepA protein of plasmid RSF1010 is a replicative DNA helicase, *J. Biol. Chem. 272*, 30228$-$30236.
4. Roleke, D., Hoier, H., Bartsch, C., Umbach, P., Scherzinger, E., Lurz, R., and Saenger, W. (1997) Crystallization and preliminary crystallographic and electron microscopy study of bacterial DNA helicase (RSF1010 RepA), *Acta Crystallogr., Sect. D 53*, 213$-$216.

5. Niedenzu, T., Roleke, D., Bains, G., Scherzinger, E., and Saenger, W. (2001) Crystal structure of the hexameric helicase RepA of plasmid RSF1010, *J. Mol. Biol. 306*, 479−487.
6. Xu, H., Frank, J., Holzwarth, J. F., Saenger, W., and Behlke, J. (2000) Interaction of different oligomeric states of hexameric DNA−helicase RepA with single-stranded DNA studied by analytical ultracentrifugation, *FEBS Lett. 482*, 180−184.
7. Xu, H., Frank, J., Trier, U., Hammer, S., Schroder, W., Behlke, J., Schafer-Korting, M., Holzwarth, J. F., and Saenger, W. (2001) Interactions of fluorescence labeled single-stranded DNA with hexameric DNA−helicase RepA: A photon and fluorescence correlation spectroscopy studies, *Biochemistry 40*, 7211−7218.
8. Xu, H., Frank, J., Niedenzu, T., and Seanger (2000) DNA helicase RepA: Cooperative ATPase activity and binding of nucleotides, *Biochemistry 39*, 12225−12233.
9. Jezewska, M. J., and Bujalowski, W. (1996) Global conformational transitions in *E. coli* primary replicative DnaB protein induced by ATP, ADP, and single-stranded DNA binding, *J. Biol. Chem. 271*, 4261−4265.
10. Bujalowski, W., Klonowska, M. M., and Jezewska, M. J. (1994) Oligomeric structure of *Escherichia coli* primary replicative helicase DnaB protein, *J. Biol. Chem. 269*, 31350−31358.
11. Egelman, E. H., Yu, X., Wild, R., Hingorani, M. M., and Patel, S. S. (1995) Bacteriophage T7 helicase/primase proteins form rings around single-stranded DNA that suggest a general structure for hexameric helicases, *Proc. Natl. Acad. Sci. U.S.A. 92*, 3869−3873.
12. Dong, F., Gogol, E. P., and von Hippel, P. H. (1995) The Phage T4-coded DNA replication helicase (gp41) forms a hexamer upon activation by nucleoside triphosphate, *J. Biol. Chem. 270*, 7462−7473.
13. Patel, S. S., and Picha, K. M. (2000) Structure and function of hexameric helicases, *Annu. Rev. Biochem. 69*, 651−697.
14. Bujalowski, W., and Klonowska, M. M. (1993) Negative cooperativity in the binding of nucleotides to *Escherichia coli* replicative helicase DnaB protein. Interactions with fluorescent nucleotide analogs, *Biochemistry 32*, 5888−5900.
15. Lohman, T. M., and Bjornson, K. P. (1996) Mechanisms of helicase-catalyzed DNA unwinding, *Annu. Rev. Biochem. 65*, 169−214.
16. von Hippel, P. H., and Delagoutte, E. (2002) Helicase mechanisms and the coupling of helicases within macromolecular machines. Part I: Structures and properties of isolated helicases, *Quart. Rev. Biophys. 35*, 431−478.
17. von Hippel, P. H., and Delagoutte, E. (2003) Helicase mechanisms and the coupling of helicases within macromolecular machines. Part II: Integration of helicases into cellular processes, *Quart. Rev. Biophys. 36*, 1−69.
18. Hingorani, M. M., and Patel, S. S., (1996) Cooperative interactions of nucleotide ligands are linked to oligomerization and DNA binding in bacteriophage T7 gene 4 helicases, *Biochemistry 35*, 2218−2228.
19. Lohman, T. M., and Bujalowski, W. (1991) Thermodynamic methods for model-independent determination of equilibrium binding isotherms for protein−DNA interactions: Spectroscopic approaches to monitor binding, *Methods Enzymol. 208*, 258−290.
20. Jezewska, M. J., and Bujalowski, W. (1996) A general method of analysis of ligand binding to competing macromolecules using the spectroscopic signal originating from a reference macromolecule. Application to *Escherichia coli* replicative helicase DnaB protein−nucleic acid interactions, *Biochemistry 35*, 2117−2128.
21. Jezewska, M. J., Kim, U.-S., and Bujalowski, W. (1996) Interactions of *Escherichia coli* primary replicative helicase DnaB protein with nucleotide cofactors, *Biophys. J. 71*, 2075−2086.
22. Jezewska, M. J., and Bujalowski, W. (1997) Quantitative analysis of ligand−macromolecule interactions using differential quenching of the ligand fluorescence to monitor the binding, *Biophys. Chem. 64*, 253−269.
23. Bujalowski, W., and Jezewska, M. J. (2000) *Spectrophotometry and Spectrofluorimetry. A Practical Approach* (Gore, M. G., Ed.) pp 141−165, Oxford University Press, New York.
24. Edelhoch, H. (1967) Spectroscopic determination of tryptophan and tyrosine in proteins, *Biochemistry 6*, 1948−1954.
25. Gill, S. C., and von Hippel, P. H. (1989) Calculation of protein extinction coefficients from amino acid sequence data, *Anal. Biochem. 182*, 319−326.
26. Bujalowski, W., and Jezewska, M. J. (1995) Interactions of *Escherichia coli* primary replicative helicase DnaB protein with single-stranded DNA. The nucleic acid does not wrap around the protein hexamer, *Biochemistry 34*, 8513−8519.
27. Jezewska, M. J., Kim, U.-S., and Bujalowski, W. (1996) Binding of *Escherichia coli* primary replicative helicase DnaB protein to single-stranded DNA. Long-range allosteric conformational changes within the protein hexamer, *Biochemistry 35*, 2129−2145.
28. Bujalowski, W., and Klonowska, M. M. (1994) Structural characteristics of the nucleotide binding site of the *E. coli* primary replicative helicase DnaB protein. Studies with ribose and base-modified fluorescent nucleotide analogs, *Biochemistry 33*, 4682−4694.
29. Bujalowski, W., and Klonowska, M. M. (1994) Close proximity of tryptophan residues and ATP-binding site in *Escherichia coli* primary replicative helicase DnaB protein. Molecular topography of the enzyme, *J. Biol. Chem. 269*, 31359−31371.
30. Bujalowski, W., and Klonowska, M. M. (1993) Negative cooperativity in the binding of nucleotides to *Escherichia coli* replicative helicase DnaB protein. Interactions with fluorescent nucleotide analogs, *Biochemistry 32*, 5888−5900.
31. Hill, T. L. (1985) *Cooperativity Theory in Biochemistry. Steady State and Equilibrium Systems*, pp 167−234, Springer-Verlag, New York.
32. Galletto, R., Jezewska, M. J., and Bujalowski, W. (2003) Interactions of the *Escherichia coli* DnaB helicase hexamer with the replication factor the DnaC protein. Effect of nucleotide cofactors and the ssDNA on protein−protein interactions and the topology of the complex, *J. Mol. Biol. 329*, 441−465.
33. Jezewska, M. J., Rajendran, S., and Bujalowski, W. (1997) Strand specificity in the interactions of *Escherichia coli* primary replicative helicase DnaB protein with replication fork, *Biochemistry 36*, 10320−10326.
34. Jezewska, M. J., Rajendran S., Bujalowska, D., and Bujalowski, W. (1998) Does ssDNA pass through the inner channel of the protein hexamer in the complex with the *E. coli* DnaB helicase? Fluorescence energy transfer studies, *J. Biol. Chem. 273*, 10515−10529.
35. Jezewska, M. J., Rajendran, S., and Bujalowski, W. (1998) Complex of *Escherichia coli* primary replicative helicase DnaB protein with a replication fork. Recognition and structure, *Biochemistry 37*, 3116−3136.
36. Bujalowski, W., and Jezewska, M. J. (2000) Kinetic mechanism of the single-stranded DNA recognition by *Escherichia coli* replicative helicase DnaB protein. Application of the matrix projection operator technique to analyze stopped-flow kinetics, *J. Mol. Biol. 295*, 831−852.
37. Wong, I., and Lohman, T. (1992) Allosteric effects of nucleotide cofactors on *Escherichia coli* Rep helicase−DNA binding, *Science 256*, 350−355.
38. Pang, P. S., Jankowsky, E., Planet, P., and Pyle, A. M. (2002) The hepatitis C viral NS3 protein is a processive DNA helicase with cofactor enhanced RNA unwinding, *EMBO J. 21*, 1168−1176.
39. Picha, K. M., and Patel, S. S. (1998) Bacteriophage T7 DNA helicase binds dTTP, forms hexamers, and binds DNA in the absence of Mg^{2+}. The presence of dTTP is sufficient for hexamer formation and DNA binding. *J. Biol. Chem. 273*, 27315−27319.
40. Record, M. T., Lohman, T. M., and deHaseth, P. L. (1976) Ion effects on ligand−nucleic acid interactions, *J. Mol. Biol. 107*, 145−158.
41. Record, M. T., Jr., Anderson, C. F., and Lohman, T. M. (1978) Thermodynamic analysis of ion effects on the binding and conformational equilibria of proteins and nucleic acids: The roles of ion association or release, screening, and ion effects on water activity, *Quart. Rev. Biophys*. 11, 103−178.
42. Garfinkel, L., and Garfinkel, D. (1984) Calculation of free-Mg^{2+} concentration in adenosine 5′-triphosphate containing solutions *in vitro* and *in vivo*, *Biochemistry 23*, 3547−3552.
43. Jencks, W. P. (1981) On the attribution and additivity of binding energies, *Proc. Natl. Acad. Sci. U.S.A.* 78, 4046−4050.
44. Jencks, W. P. (1980) The utilization of the binding energy in coupled vectorial processes, *Adv. Enzymol. 51*, 75−106.
45. Rajendran, S., Jezewska, M. J., and Bujalowski, W. (2000) Multiple-step kinetic mechanism of DNA-independent ATP binding and hydrolysis by *Escherichia coli* replicative helicase DnaB protein: Quantitative analysis using the rapid quench-flow method, *J. Mol. Biol. 303*, 773−795.

BI048036H